5.6 Discussion

Although the number of 52 SAR images, corresponding with 26 analyzed interferograms, is certainly not enough to provide sufficient information for a thorough statistical analysis, it may be useful to summarize the observed effects in a more systematic way. The database of SAR images covers nearly every month of the year, see the histogram in figure 5.153, except January. Therefore, all seasons have been sampled. Unfortunately, the limited duration of the ERS tandem mission does not permit a longer series of interferograms over one particular area. A consequence of the orbit configuration is that the diurnal cycle of the weather is only sampled at one nearly discrete time instant for every image. Therefore, the imaging times are always approximately 21:40 UTC for the *Flevoland ascending* interferograms, and about 10:30 UTC for all other interferograms. Variations between daytime and nighttime acquisitions could therefore not be studied.

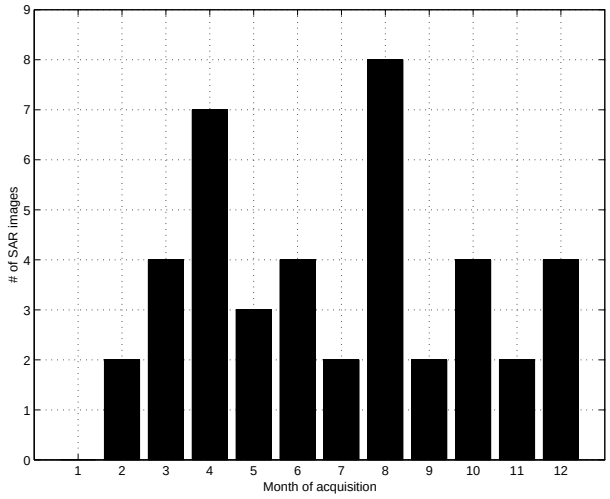

Figure 5.153 *Histogram showing the number of analyzed SAR images, ordered by the month of acquisition.*

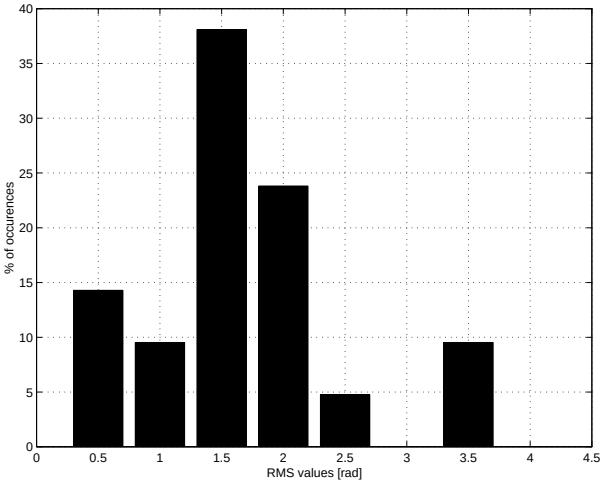

Figure 5.154 *Histogram showing the rms values of the interferograms in the database and the frequencies of occurrence*

A review of the observed rms phase values is shown in table 5.22. The rms values vary between 0.6 rad for interferogram gd4, and 3.6 rad for interferogram fa2. Note that the interpretation of the rms values is dependent on the area used for its calculation. For each of the 5 interferogram locations studied, the decorrelated areas (mainly water) varied in spatial coverage, and the combination of two interferograms in the *Flevoland ascending* series enabled a much larger surface for evaluation.

Figure 5.154 shows the percentages of occurrence for the rms values, in eight categories. Root mean square values around 1.5 rad occur the most frequently in this series. Ordering the observed rms values based on the month of acquisition produces the histogram in figure 5.155. The months May and July have in this database phase variations with an rms which is double of the values observed in all other interferograms. Naturally, this is a consequence of only one or two interferograms, and it can therefore not be used for the derivation of general rules. However, it can be expected that 'summer'-thunderstorms, which occur often in this region, will produce strong phase artifacts in corresponding interferograms.

ID	rms (rad)	class	cloud	waves	striation	localized anomalies	keyword
gd1	3.4	D	Cb		yes	yes	cells
gd2	1.5	B			yes	yes	pearls
gd3	1.6	C					dog ear
gd4	0.6	A		yes	yes		x-waves
gd5	1.4	B		yes	yes	yes	
gd6	1.8	C	Cu		yes	yes	cells
gd7	1.8	C	Cu		yes	yes	cells
gdex2	1.9	C		yes		yes	corner
cd1	1.0	B	Cb		yes	yes	cells
fd1	1.7	C	Cu		yes	yes	bean,cells
fd2	1.3	B	Cu	yes		yes	cells
fd3	1.3	B				yes	gradient
fd4	1.8	C	Cb			yes	cells
fd5	0.7	A				yes	
fd6	0.5	A		yes	yes		
fd7	1.7	B	Cu	yes	yes	yes	cells
fa1	2.0	C	Cu			yes	cells,intrusion
fa2	3.6	D	Cb			yes	sickle,line,cells
fa3	2.5	C		yes		yes	ramp
fa4	1.3	B				yes	intrusion
fa5	1.2	B		yes		yes	cells

Table 5.22 *Statistics and observations in the interferograms. The rms values are listed, as well as the magnitude class, see table 5.23. Only cumulus or cumulonimbus clouds are indicated in the cloud category. Waves are observed mostly at small parts of the image. Striation indicates clear anisotropic behavior of the observed patterns. Localized anomalies are defined as artifacts with a spatial extent of 20 km or less, and a phase disturbance of 2 rad or more. The keyword column describes special features of the interferogram.*

5.6.1 Classification of the observed effects

A classification of the observed effects can be based on the magnitude and the type and scale of the disturbance. Based on the *magnitude*, four classes are defined based on the observed rms values. The rms values are regarded to be representative for a Gaussian distribution, and can be used to find the 95% range of the distribution. The classes, labeled A, B, C, and D, are listed in table 5.23, together with the percentage of the analyzed interferograms which fall in this range. Table 5.22 indicates for each interferogram to what category it belongs.

Based on the *type* of disturbance, *localized anomalies* are defined as those disturbances which occur on a spatial scale of less than 20 km, and have a magnitude of more than 2 radians. Within this definition, 17 of the 21 (combined) interferograms displayed this type of artifacts. These interferograms are listed in table 5.22. Furthermore, in the table it is shown if wave effects are observed. Waves have been observed perpendicular as well as parallel to the wind direction at some heights. These effects are mostly localized, and

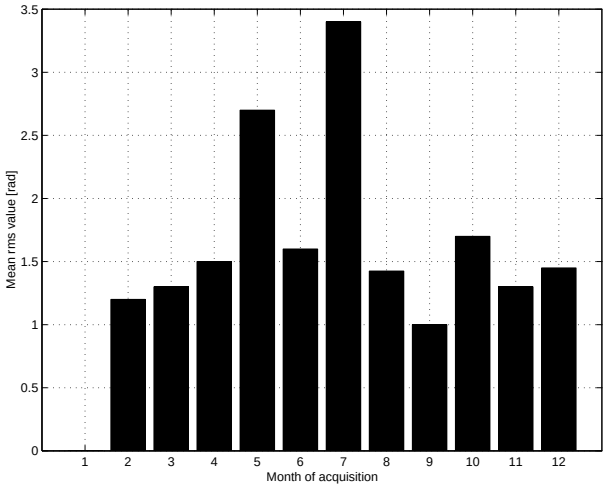

Figure 5.155 *Histogram showing the mean rms values, ordered by the month of acquisition*

Class	rms (rad)	95% range (rad)	Percentage
A	$< \pi/4$	$[0, \pi]$	14%
B	$[\pi/4, \pi/2]$	$[\pi, 2\pi]$	38%
C	$[\pi/2, \pi]$	$[2\pi, 4\pi]$	38%
D	$\pi <$	$[4\pi, \infty]$	10%

Table 5.23 *Classification of the magnitude of atmospheric disturbance.*

relatively small. Wave effects are observed in 8 of the 21 interferograms. Another effect is *striation*—where almost the whole interferogram is covered by a pattern with a clear orientation. Sometimes these effects could be defined as moisture transport in a more or less laminar flow. The possibility to find an orientation in the effects occurred in 10 of the 21 interferograms. Finally, one or two *keywords* have been chosen, which reflect the peculiarities of a specific interferogram. *Cells* occur most often, and indicate localized phase artifacts, which are quite discernible from the background. *Pearls* is a keyword for the 'string of pearls' effect, where a pattern is formed by many small circular anomalies, often aligned in a certain direction. The *dog ear* is specific for gd3, and shows a peculiar anomaly in the corner of the interferogram. The effect labeled *x-waves* shows wave-like effects in more than on direction. All other keywords refer to the shape of the observed anomalies.

An interesting relation is found by listing all the observations of cumulus or cumulonimbus clouds in table 5.22. It appears that in all cases in which these cloud types were observed, *cells* were observed in the interferogram. From this observation, it may be concluded that this type of cloud cover indicates strong local variations in relative humidity, which has a considerable influence on the SAR interferograms.

Chapter 6

Conclusions and recommendations

6.1 Conclusions

In this study, a series of 26 SAR interferograms is analyzed in order to assess the influence of atmospheric heterogeneities on the interferometric phase observations from the ERS tandem mission. This report gives a brief summary of the current understanding of signal delay induced by the Earth's atmosphere, and its effect on repeat pass SAR interferometry. It describes the characteristics of the used interferometric and meteorologic database, and systematically covers the analyses of all interferograms. Based on this work, the following conclusions can be drawn.

6.1.1 The scale and magnitude of the observed effects

Atmospheric influences have been observed in each of the 26 interferograms. The observed spatial scales reach from hundreds of meters to 100–200 km. For scales reaching the full image size, it is, however, difficult to discern them from errors in the satellite orbits.

The magnitude of the effects can be expressed in an rms value, or in the extreme values observed in the interferogram. Observed rms values, taken over a significant part of the image, reach from 0.5–3.6 radians. Assuming a Gaussian distribution, this implies that 95% of the observed phase values varies over a minimal range of 0.3 phase cycles up to a maximal range of 2.3 phase cycles. Extreme ranges of 4 phase cycles are found during thunderstorms at the two SAR acquisitions.

Note that the degree of coherence was found to be sufficient (> 0.7) for all land areas in the interferograms.

6.1.2 A classification of effects

Analyzing the series of interferograms, it became apparent that every interferogram displayed a totally different atmospheric behavior. Nevertheless, it is tried to sort the observed atmospheric disturbance in different categories. First, *isolated anomalies* are found in 18 of the 21 (combined) interferograms. Isolated anomalies are defined here as anomalies with a spatial extent of 20 km or less, and a phase disturbance of 2 radians or more. Secondly, *striation* is observed in 10 interferograms. Striation refers to a pattern of linear features over a significant portion of the interferogram, often connected with transport of moisture. The effect may be equal over the whole interferogram, or change gradually from a more laminar to a turbulent flow. A third category is formed by *wave effects*. The

waves are mostly observed in only a part of the interferogram, and can be often identified as gravity waves or cloud/moisture streets. The amplitude is mostly less than 1 phase cycle. *Frontal zones* form a fourth category. Different effects have been observed, from smooth gradients in the phase, to a very distinct 'wave crest' with a wavelength of just some 5 kilometers. Finally, *overall atmospheric variation* is observed in many of the interferograms. This is phase variation of a limited magnitude, and with varying wavelengths, perhaps best described as a 'bumpy' surface. This effect might be closely connected with turbulent behavior of air and its constituents.

6.1.3 The driving mechanisms

Atmospheric signal in SAR interferograms is due to localized changes in the refractive index of the medium. Changes in the refractive index can be caused by more parameters than only pressure, temperature and water vapor. Using the weather radar, it seems that also rain fall can influence the refractive index, resulting in severe phase shifts in the interferogram. In most of the cases the spatial variation of pressure and temperature is not large enough to cause strong localized phase gradients in the 100×100 km interferograms. Their effects will cause gradients over the whole interferogram, which are difficult to discern from, e.g., orbit uncertainties. The localized spatial behavior of humidity is believed to be dominant in causing atmospheric signal in the interferograms.

No identifiable ionospheric effects have been found in this series of interferograms. For all interferograms, reasonable explanations for the observed effects could be provided using only variation in tropospheric parameters.

6.1.4 The use of meteorological information

In general, two types of meteorological data can be distinguished in this context. First, near-instantaneous observations (weather radar, cloud observations, weather observations, coinciding high resolution satellite imagery) at the time of the SAR acquisitions can give an indication for the type, size and magnitude of the disturbances to be expected. Secondly, more general meteorological information, such as daily weather charts, weather model data, and some satellite imagery can be used to express the likelihood of some types of atmospheric disturbance in SAR interferograms.[1]

Weather radar observations of precipitation correlate in most cases closely with observed anomalies in the interferograms. This fact, and the nearly continuous operation of the weather radar over this area yield possibilities for at least an identification tool for strong localized artifacts. Further study is needed to assess the relationship between the observations of both instruments, which might lead to algorithms to suppress the interferometric artifacts using weather radar information.

Meteorological information from current *satellite imagery* can be useful for the detection of storm fronts, or regions of strong atmospheric instability. However, the temporal and spatial sampling rates pose the main limitations for this type of observations. Much of the strong disturbance in interferograms can be observed within small spatial ranges, e.g., less than 10 km. The resolution of Meteosat and AVHRR is too coarse to observe this, although AVHRR gives already some better quality when combining the different

[1] A short overview on the use of meteorological information is given in Hanssen et al. (1998b)

channels. Temporal sampling is the second limitation. Whereas a geostationary satellite such as Meteosat provides an image every half hour, AVHRR resamples every six hours. This implies that the time difference between the SAR acquisition and the nearest AVHRR acquisition varies between 1 and 3 hours, which is often too long to interpret the state of the atmosphere. If, however, spaceborne meteo-observations are available, the most important features to look for are strong convective clouds (cumulonimbus), strong and short water vapor gradients, and wave patterns.

Synoptic observations can be used to get an overview of the meteorological situation during a SAR acquisition. An advantage of this type of observations is that they are regularly acquired (every hour) over a large number of observation stations, and that the observations are coded in an internationally consistent way. Apart from the automatic observations, especially the manual observations can be of great significance. Manual observations include cloud type, cloud cover, cloud heights, and weather category. It has been shown that often the most disturbing *localized anomalies* in the interferometric phase can be connected to convective cloud development, i.e. clouds of the *cumulus* and *cumulonimbus* genus.

Daily national or regional *weather charts* give a first impression of the dynamics of the weather during the day in which a SAR image was acquired. Naturally, this is only of very limited use to assess the amount of disturbance in an interferogram. It may, however, be useful if one needs to select from a series of acquisitions over a specific area. Especially precipitation or cloud cover measures can be routinely used to either select or reject a specific image from a series.

Apart from the information obtained from additional meteorological data sources, information on the atmospheric status can sometimes be obtained from the *backscatter* over water areas, see Hanssen et al. (1998a). Especially information on the wind direction and velocity, footprints of rain cells, or boundary layer vortices can be available from single SAR images, and be used as a priori information on the expected atmospheric signal in the interferogram.

Table 6.1 shows a generalized overview of the characteristics and estimated availability of different meteorological observations.

Method	Spatial res.	Temp. res.	Type of effect	Availability
Synoptic	[30 × 30]	[0.5–1]	clouds fronts	medium
Weather radar	[0.5 × 0.5]	[0.25]	precip	hard
Radio sondes	[100 × 100]	[6–12]	waves	medium
Spaceborne:				
geostat:	[5 × 5]	[0.5]	fronts convection	good
orbiting:	[1 × 1]	[6]	clouds	good
Weather charts	[50 × 50]	[24]	fronts	good

Table 6.1 *The use of historical meteorological data: average spatial and temporal resolution, type of effect, and estimate of availability.*

6.1.5 Some rules of thumb

Although the amount of investigated situations is certainly not sufficient to give statistical estimates, some general rules of thumb can be given based on the experience obtained here and the knowledge of general atmospheric dynamics.

- Winter acquisitions are expected to be more stable in terms of atmospheric disturbance than summer and especially autumn acquisitions. This is due to the fact that cold air cannot hold that much water vapor, and that convection is usually less extreme.
- The convective layer is usually more active during daytime. During nighttime there is a residual layer and a stable boundary layer. Therefore, it can be expected that nighttime SAR acquisitions show less atmospheric disturbance due to convection than daytime acquisitions. For the ERS orbits, this implies that ascending orbits are prefered over descending orbits.

On the handling of atmospheric signal

Generally, there are two ways for treating atmospheric disturbance in SAR interferograms: *selection* or *statistical suppression*. This study has been focussed on selection, assuming that either only two SAR images are available[2] and it is necessary to get estimates of the amount and characteristics of the atmospheric artifacts, or that the tandem interferogram is not processed yet, and an a priori statement on the amount of disturbance to be expected is desired.

Convective processes are most likely to be detected in interferograms, especially when more than one interferometric pair is evaluated. Therefore, a procedure of averaging interferograms (*statistical suppression*) is cumbersome for these effects, since many interferograms are necessary for eliminating these strong and isolated effects. For the interferometric characteristics of *overall atmospheric variation*, stacking and averaging interferograms is more likely to have good results, since the spectral characteristics are comparable in more interferograms. The same holds for the wave effects.

6.1.6 Meteorological relevance

Interferometric signal delay maps can be useful for further study and for the understanding of atmospheric water vapor distribution and the relative amounts of precipitable water in clouds. Especially the combination of the high resolutions, starting from 20×20 m, the nearly instantaneous data acquisitions, and the accuracies, can help provide new insights in atmospheric dynamics. The large database of tandem SAR images acquired over the world contains a wealth of information for scientific research in this field.

6.2 Recommendations

6.2.1 On the assimilation of meteorological observation with SAR interferometry

The relationship between coded manual synoptic observations and the interferometric phase anomalies suggests a potential for an automatic evaluation system. Possibilities to

[2]This is often the case for ERS tandem interferograms, since temporal decorrelation over longer times hampers an evaluation of a series of interferograms

obtain these synoptic observations for a specific region in the world using the Internet need to be studied. Global or regional meteorologic organizations could be of assistance in this respect.

6.2.2 The elimination of the effects

Temporally coincident quantitative observations by weather radar could be further analyzed and compared with observed phase delays in the interferograms. Establishing a functional relation between both types of observations is a first step towards elimination of localized anomalies in the SAR interferograms.

6.2.3 The quantification of the effects

Since rms values can be determined using areas of different spatial extent, the effect of localized but strong anomalies will differ depending on the area used for evaluation. Especially since errors in distinguishing topographic from atmospheric signal will be significant for localized strong anomalies in combination with relatively short baselines, more specialized error measures need to be used to describe the observed atmospheric disturbance signal.

6.2.4 The use of meteorological data

Since atmospheric phenomena as rain, cold fronts and water vapor distribution have been found the main sources of interferometric disturbance, climatological/meteorological statistical information on a specific area can be valuable to assess the possibilities and type of atmospheric disturbance to be expected. Information on cloud types and frequencies of occurrence are often available as a function of the time of year, which can give some a priori information on a specific area. The same holds for rain statistics and general atmospheric activity.

6.2.5 The ERS SAR tandem archive

As described in paragraph 6.1.6, the archive of potential ERS tandem interferograms, in combination with reference elevation models, contains a wealth of information for the atmospheric sciences. An active promotion of this new application of SAR interferometry is needed to inform the scientific community of these possibilities.

6.2.6 Münchhausens bootstrap

Baron von Münchhausen pulled himself and his horse out of a swamp by pulling his own bootstrap. The story shows the inherent connection—and paradox—of one action (to pull) with another (to be pulled). An equivalent reasoning holds in my opinion for the different effects in repeat pass SAR interferograms, there is an inherent connection between the different types of signals which are merged in the interferometric phase. In recent studies on atmospheric effects in SAR interferometry, mostly terms as atmospheric *disturbance* or *artifacts* were used. Based on the experience from this work, I propose to regard the influence of the atmosphere on SAR interferometry as a mature signal, and to refer to it in future publications as atmospheric *signal*.

Bibliography

Afraimovich, E. L., Terekhov, A. I., Udodov, M. Y. and Fridman, S. V. (1992), Refraction distortions of transionospheric radio signals caused by changes in a regular ionosphere and by travelling ionospheric disturbances, *Journal of Atmospheric and Terrestrial Physics*, **54**(7/8):1013–1020.

Alber, C., Ware, R., Rocken, C. and Solheim, F. (1997), GPS surveying with 1 mm presision using corrections for atmospheric slant path delay, *GRL*, **24**(15):1859–1862.

Askne, J. and Nordius, H. (1987), Estimation of tropospheric delay for microwaves from surface weather data, *Radio Science*, **22**:379–386.

Bean, B. R. and Dutton, E. J. (1986), *Radio Meteorology*, Dover, New York.

Bevis, M., Businger, S., Herring, T. A., Anthes, R. A., Rocken, C. and Ware, R. H. (1994), GPS meteorology: mapping zenith wet delays onto precipitable water, *Journal of Applied Meteorology*, **33**(3).

Bevis, M., Businger, S., Herring, T. A., Rocken, C., Anthes, R. A. and Ware, R. H. (1992), GPS Meteorology: Remote sensing of atmospheric water vapor using the Global Positioning System, *Journal of Geophysical Research*, **97**:15,787–15,801.

Bevis, M., Chiswell, S., Businger, S., Herring, T. A. and Bock, Y. (1996), Estimating wet delays using numerical weather analysis and predictions, *Radio Science*, **31**(3):477–487.

Born, M. and Wolf, E. (1980), *Electromagnetic Theory of Propagation Interference and Diffraction of Light*, Permagon Press, New York.

Campen, C. F., Cole, A. E., Condron, T. P., Ripley, W. S., Sissenwine, N. and Solomon, I., eds. (1960), *Handbook of Geophysics*, MacMillan, New York.

Cheng, K. and Huang, Y.-N. (1992), Ionospheric disturbances observed during the period of Mount Pinatubo eruptions in June 1991, *Journal of Geophysical Research*, **97**(A11):16,995–17,004.

Costantini, M. (1996), A Phase Unwrapping Method Based on Network Programming, in: *Fringe 96, Zürich, Switzerland.*

Crane, R. K. (1996), *Electromagnetic wave propagation through rain*, John Wiley & Sons, Inc., New York.

Darling, A. and Mongeon, A. (1996), Meteorological Codes, National Weather Service, http://www.nws.noaa.gov/code.shtml.

Davis, J., Elgered, G., Niell, A. and Kuehn, C. (1991), Ground-based measurement of gradients in the "wet" radio refractivity of air, *Radio Science*, **28**:1003–1018.

Davis, J. L., Herring, T. A., Shapiro, I. I., Rogers, A. E. E. and Elgered, G. (1985), Geodesy by radio interferometry: Effects of atmospheric modelling errors on estimates of baseline length,

Radio Science, **20**(6):1593–1607.

Delacourt, C., Briole, P., Achache, J., Fruneau, B. and Carnec, C. (1997), Correction of the tropospheric delay in SAR interferometry and application to 1991-93 eruption of Etna volcano, Italy, in: *AGU Fall meeting, December 8-12, San Francisco, USA,*.

Duchossois, G., Kohlhammer, G. and Martin, P. (1996), Completion of the ERS Tandem Mission, *Earth Observation Quarterly*, **55**.

Dupont, S., Nonin, P., Renouard, L., Pichon, G. and Bignone, F. (1997), Atmospheric artifacts in ERS DTM. ISTAR's experience over multiple sites and large areas, in: *Proc. of the third ERS symposium, Florence, Italy, 17-20 March 1997*.

ECMWF (1994), ECMWF, *Meteorological Bulletin*, **M3.2**.

Edgar, A. K., Dodsworth, E. J. and Warden, M. P. (1973), The design of a modern surveillance radar, in: *Int. Conf. Radar–Present and Future, IEE Conf.Pub.,no. 105, 23–25 Oct. 1973*, pp. 8–13.

Eineder, M. and Adam, N. (1997), A Flexible System for the Generation of Interferometric SAR Products, in: *International Geoscience and Remote Sensing Symposium, Singapore,3–8 August 1997*.

Elliot, W. P. and Gaffen, D. J. (1991), On the utility of radiosonde humidity archives for climate studies, *Bulletin of the American Meteorological Society*, **72**:1507–1520.

Frisch, U. (1995), *Turbulence: the legacy of A.N. Kolmogorov*, University Press, Cambridge.

Ghiglia, D. C. and Romero, L. A. (1994), Robust two-dimensional weighted and unweighted phase unwrapping that uses fast transforms and iterative methods, *J. Opt.Soc.Am.A*, **11**(1):107–117.

Goldhirsch, J. and Rowland, J. R. (1982), A Tutorial Assessment of Atmospheric Height Uncertainties for High-Precision Satellite Altimeter Missions to Monitor Ocean Currents, *IEEE Trans. on Geoscience and Remote Sensing*, **GE-20**(4):418–434.

Goldstein, R. (1995), Atmospheric limitations to repeat-track radar interferometry, *Geophysical Research Letters*, **22**(18):2517–2520.

Hall, M. P. M., Barclay, L. W. and Hewitt, M. T., eds. (1996), *Propagation of Radiowaves*, The Institution of Electrical Engineers, London.

Hanssen, R. (1996), GISARE: GPS metingen voor de schatting van atmosferische parameters, *GPS Nieuwsbrief*, **11**(1):17–21.

Hanssen, R. and Feijt, A. (1996), A first quantitative evaluation of atmospheric effects on SAR interferometry, in: *'Fringe 96' workshop on ERS SAR Interferometry, 30 Sep – 2 Oct, Zürich, Switzerland*, pp. 277–282, ESA SP-406.

Hanssen, R., Lehner, S. and Weinreich, I. (1998a), Atmospheric Heterogeneities from - ERS tandem SAR Interferometry and Sea Surface Images, in: *CEOS SAR Workshop, ESTEC, Noordwijk, The Netherlands, 3-6 February 1998*, pp. 33–39.

Hanssen, R. and Usai, S. (1997), Interferometric phase analysis for monitoring slow deformation processes, in: *3rd ERS Symp. on Space at the service of our Environment, Florence, Italy, 17–21 March 1997*, ESA SP-414, pp. 487–491.

Hanssen, R., Zebker, H., Klees, R. and Barlag, S. (1998b), On the use of meteorological observations in SAR interferometry, in: *International Geoscience and Remote Sensing Symposium, Seattle,6–10 July 1998*, pp. 1644–1646.

Ho, C. M., Mannucci, A. J., Lindqwister, U. J., Pi, X., Tsurutani, B. T., Sparks, L., Iijima, B. A., Wilson, B. D., Harris, I. and Reyes, M. J. (1998), Global ionospheric TEC variations during January 10, 1997 storm, *GRL*, **25**(14):2589–2592.

Hopkins, E. J. (1996), Weather and Climate: RADIOSONDES – An Upper Air Probe, http://www.meteor.wisc.edu/~hopkins/aos100/wxi-raob.htm, University of Wisconsin.

Jakowski, N., Bettac, H. D. and Jungstand, A. (1992), Ionospheric corrections for Radar Altimetry and Geodetic Positioning Techniques, in: *Proc. of the Symp. Refraction of Transatmospheric Signals in Geodesy, the Hague, 19–22 may 1992*, pp. 151–154.

Kooij, M., van Halsema, D., Groenewoud, W., Mets, G. J., Overgaauw, B. and Visser, P. (1995), *SAR Land Subsidence Monitoring*, BCRS.

van Lammeren, A., Russchenberg, H., Apituley, A. and Feijt, A. (1997), CLARA: a data set to study sensor synergy, in: *Proc. of the workshop on Synergy of Active Instruments of the Earth Radiation Mission, November 12-14, GKSS Research Center, Geesthacht, Germany.*

Li, F. K. and Goldstein, R. M. (1990), Studies of Multibaseline Spaceborne Interferometric Synthetic Aperture Radars, *IEEE Trans. on Geoscience and Remote Sensing*, **28**(1):88–97.

Mason, B. J. (1971), *The Physics of Clouds*, University Press, Oxford, 2nd edn.

Massonnet, D., Briole, P. and Arnaud, A. (1995), Deflation of Mount Etna monitored by spaceborne radar interferometry, *Nature*, **375**:567–570.

Massonnet, D. and Feigl, K. L. (1995), Discrimination of geophysical phenomena in satellite radar interferograms, *Geophysical Research Letters*, **22**(12):1537–1540.

Massonnet, D., Rossi, M., Carmona, C., Adagna, F., Peltzer, G., Feigl, K. and Rabaute, T. (1993), The displacement field of the Landers earthquake mapped by radar interferometry, *Nature*, **364**(8):138–142.

McIlveen, R. (1995), *Fundamentals of Weather and Climate*, Chapman and Hall, London, 2nd edn.

Nathanson, F. E. (1969), *Radar design principles*, McGraw-Hill.

Niell, A. E. (1996), Global mapping functions for the atmosphere delay at radio wavelengths, *Journal of Geophysical Research*, **101**(B2):3227–3246.

Parsons, D. B. (1992), An Explanation for Intense Frontal Updrafts and Narrow Cold-Frontal Rainbands, *Journal of the Atmospheric Sciences*, **49**(19):1810–1825.

Reber, E. E. and Swope, J. R. (1972), On the correlation of the total precipitable water in a vertical column and the absolute humidity at the surface, *Journal of Applied Meteorology*, **11**:1322–1325.

Rogers, D. V. and Olsen, R. L. (1975), Delay and its relation to attenuation in microwave propagation through rain, in: *USNC/URSI Annual Meeting, Boulder CO, 20–23 Oct 1975.*

Ruf, C. S. and Beus, S. E. (1997), Retrieval of Tropospheric Water Vapor Scale Height from Horizontal Turbulence Structure, *IEEE Trans. on Geoscience and Remote Sensing*, **35**(2):203–211.

Saastamoinen, J. (1972), Introduction to Practical Computation of Astronomical Refraction, *Bulletin Geodesique*, **106**:383–397.

Schättler, B. (1997), Personal communication,.

Schwäbisch, M. (1995), Die SAR-Interferometrie zur Erzeugung digitaler Geländemodelle, Forschungsbericht 95-25, Deutsche Forschungsanstalt für Luft- un Raumfahrt, Oberpfaffen-

hofen.

Schwäbisch, M. and Geudtner, D. (1995), Improvement of Phase and Coherence Map Quality Using Azimuth Prefiltering: Examples from ERS-1 and X-SAR, in: *International Geoscience and Remote Sensing Symposium, Florence, Italy, 10–14 July 1995*, pp. 205–207.

Smith, Jr., E. K. and Weintraub, S. (1953), The Constants in the Equation for Atmospheric Refractive Index at Radio Frequencies, *Proceedings of the I.R.E*, **41**:1035–1037.

Solheim, F. S., Vivekanandan, J., Ware, R. H. and Rocken, C. (1997), Propagation Delays Induced in GPS Signals by Dry Air, Water Vapor, Hydrometeors and Other Particulates, *draft for J. of Geoph. Res.*

Spoelstra, T. A. T. (1997), Personal communication.

Stolk, R., Hanssen, R., van der Marel, H. and Ambrosius, B. (1997), Troposferische signaalvertraging; een vergelijking tussen GPS en SAR interferometrie, *GPS Nieuwsbrief*, **2**:3–7.

Stull, R. B. (1988), *An Introduction to Boundary Layer Meteorology*, Kluwer, Dordrecht.

Stull, R. B. (1995), *Meteorology Today For Scientists and Engineers*, West Publishing, St. Paul, Minneapolis.

Tarayre, H. (1996), *Extraction de Modeles Numeriques de Terrain par Interferometrie Radar Satellitaire: Algorithmie et Artefacts Atmospheriques*, Ph.D. thesis, Institut National Polytechnique de Toulouse, Toulouse.

Tarayre, H. and Massonnet, D. (1996), Atmospheric propagation heterogeneities revealed by ERS-1 interferometry, *Geophysical Research Letters*, **23**(9):989–992.

Tatarski, V. I. (1961), *Wave propagation in a turbulent medium*, McGraw-Hill, New York.

Tatarskii, V. I. (1971), *The Effects of the Turbulent Atmosphere on Wave Propagation*, Israel Program for Scientific Translations, Jerusalem, translated from Russian.

Topografische Dienst Nederland and Meetkundige Dienst Rijkswaterstaat (1997), TopHoogteMD Digital Elevation Model.

Treuhaft, R. N. and Lanyi, G. E. (1987), The effect of the dynamic wet troposphere on radio interferometric measurements, *Radio Science*, **22**(2):251–265.

Wessels, H. R. A. (1997), Personal communication,.

Zebker, H. A., Rosen, P. A. and Hensley, S. (1997), Atmospheric effects in interferometric synthetic aperture radar surface deformation and topographic maps, *Journal of Geophysical Research*, **102**(B4):7547–7563.

Zebker, H. A., Werner, C. L., Rosen, P. A. and Hensley, S. (1994), Accuracy of Topographic Maps Derived from ERS-1 Interferometric Data, *IEEE Trans. on Geoscience and Remote Sensing*, **32**(4):823–836.

Publications of the Delft Institute for Earth-Oriented Space Research:

97.1	Bouman, J.	A survey of global gravity models.
97.2	Bruijne, A. de	Wavelet and Radon analysis for detection of elongated structures in profile measurements.
97.3	Onselen, K. van	Quality investigation of vertical datum connection.

Request additional copies: Ms. W.G. Coops-Luijten, Delft University of Technology, Faculty of Civil Engineering and Geosciences, Thijsseweg 11, 2629 JA, Delft, The Netherlands, e-mail: deos@geo.tudelft.nl, costs: NLG 15,– (excl. postal charges).